On Annular Impinging Jets - Experimental Data Analysis

Bc. Tomáš Turek

Supervisors: Ing. Zdeněk Trávníček, CSc., Prof. Ing. Pavel Šafařík, CSc.

Abstract

The paper deals with experimental data achieved during measurement on annular impinging jets. The results of experiments are analyzed and discussed. Critical value of nozzle-to-wall distance is determined and consequences of phenomena are shown.

Keywords

Annular jet, impinging jet, bistability, hysteresis.

1. Introduction

Energy and mass transfer is an extensive task across engineering applications. Typical heat transfer applications as cooling (or heating) of surfaces are perfectly solved by the annular jet impinging on these surfaces. Recent publications show that annular impinging jets (IJs) could be used in electronics for cooling of thermally highly loaded components, Trávníček & Tesař [1, 2]; Tesař & Trávníček [3]; Trávníček et al. [4]; Maršík et al. [5]. Annular IJs jets have large potential in heat and mass transfer applications and its usage have increased lately. Therefore, many important characteristics of annular IJs (flow reattachment, bistability, hysteresis, etc.) which can influence their performance or controllability need to be clarified and identified.

An annular nozzle has a ring-shaped slit exit which is usually made by placing a centerbody into a round exit, *Figs. 1* and *2*. Moreover, this centerbody ensures that the supplied fluid through the annular nozzle is effectively utilized in contrast to a simple round nozzle which consumes a large amount of the intake fluid.

2. Experimental Setup and Methods

An experimental investigation of annular IJs near field was made at three inner/outer diameter ratios 0.84, 0.90 and 0.95. *Figure 1* shows the experiment of tested annular nozzle, the working fluid is air. The nozzle is oriented vertically upwards. The present nozzles consist of four parts: tripod, case, centerbody of the nozzle (in three variants A, B, C), and outer

Fig.1. *Arrangement of experiment.*

part. Moreover, nozzles B and C were optionally equipped with the centerbody extension. Variations of investigated nozzles and their configuration are described in *Tab. 1* and *Fig. 2*. The air flow is supplied by a compressor and kept constant by the pressure regulators and filters (regulator + filter CAMOZZI *MC202-D00*, filter CAMOZZI *MC202-F10* and regulator CAMOZZI *MC202-R10*); air is passing through the throttling valve and through the flow meter to the annular nozzle, *Fig. 2*.

The flow rate was measured by the flow meter (Rotameter AALBORG *T41T4-TA0-044-40* [6]) consisting of 4 tubes, with the range of the air volume flux *2,015-69,940*, *2,015-69,940*, *2,182-45,227*, and *791-23,742 ml/min*. Before the air enters the flow meter, pressure is taken by the manometer with the resolution of *0.1 Pa* (digital pressure meter GREISINGER *GMH 3156* with the transmitter *GMSD 2.5 BR*).

Tab. 1. *– Geometry of investigated annular nozzles.*

Nozzle	D_i [mm]	D_o [mm]	E [mm]	D_E [mm]	b [mm]	D_o/D_i	D_i/D_o
A	25.12	30.00	0.0	0.0	2.44	1.19	0.84
B	27.10	30.00	0.0	0.0	1.45	1.11	0.90
$\mathbf{B_{EXT}}$	27.10	30.00	5.0	25.0	1.45	1.11	0.90
C	28.40	30.00	0.0	0.0	0.80	1.06	0.95
$\mathbf{C_{EXT}}$	28.40	30.00	3.5	25.0	0.80	1.06	0.95

Reynolds number of the outer diameter is defined from the average exit velocity U_{AV} of jet from the annular nozzle (evaluated from the volume flow rate) by the following equations:

$$U_{AV} = 4\,Q_b/[\pi\,(D_o^2 - D_i^2)] \tag{1.1}$$

$$Re_D = U_{AV}\,D_o/\nu \tag{1.2}$$

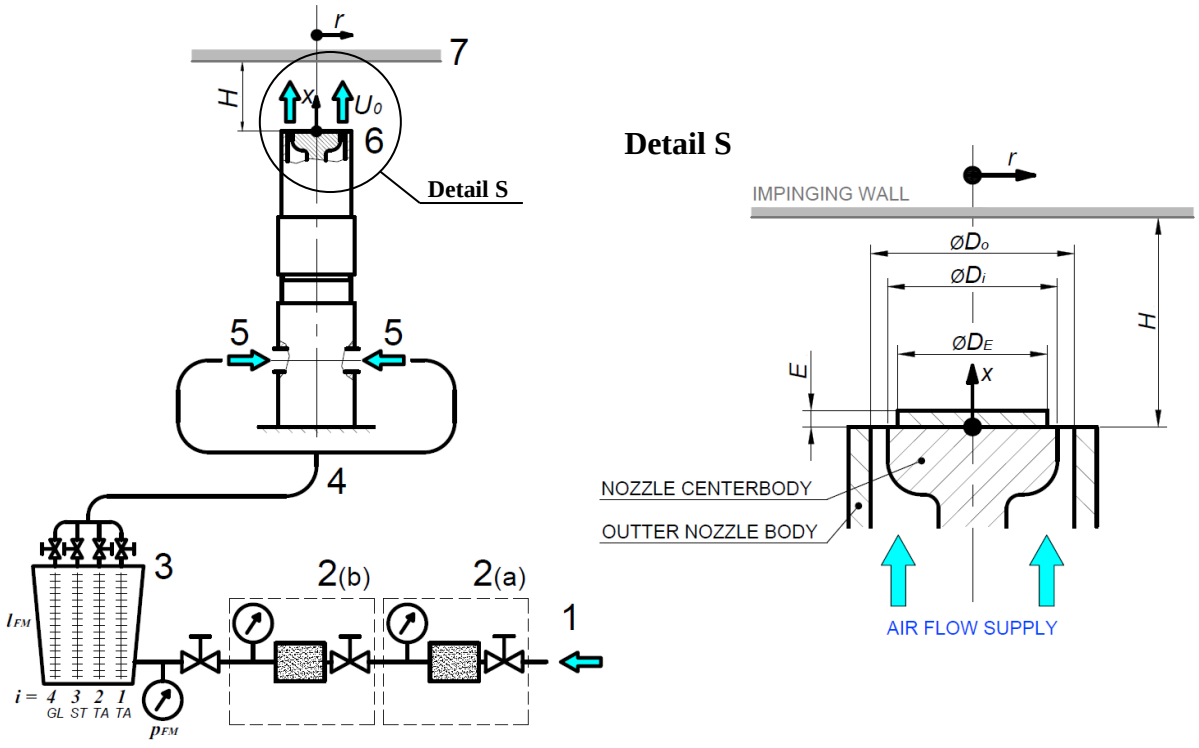

Fig.2. *Scheme of experiment: 1 – Air flow supply, 2(a), (b) – Two pressure regulators and filters, 3 – Rotameter, 4 – Flexible tubing, 5 – Pair of radial inlets, 6 – Annular nozzle, 7 – Exposed wall.*

Annular jets measurement: time-mean flow velocity is measured by the Pitot tube of outer/inner diameters *0.8* and *0.6 mm*, connected to the pressure converter - either AIRFLOW *PTSX-K1000* of range *0-1,000 Pa* with digital voltmeter or GREISINGER *GMH 3156* with the transmitter *GMSD 2.5 MR*.

Annular impinging jets measurement: wall pressure on the exposed impingement wall is measured via the hole of the diameter *0.8 mm*. The hole is connected to the manometer (second input of the GREISINGER *GMH 3156*) with the transmitter (*GMSD 2.5 MR*). The impingement has been made out of Perspex with dimensions of *220×220×2 mm*.

3. Time-Mean Flow Field

The annular jet initial region is characterized by the time-mean velocity contours in *Figs. 3* and *4*. It may be divided into the initial merging zone, the intermediate merging zone, and the fully merged zone – see Ko & Chan [7]. The initial merging zone is the region from the nozzle exit to the position at which disappears the potential core of the jet. The size of the potential core depends on the width of the annular slot: the smaller is the slot width, the smaller is the core. The mean velocity within the potential core is the same as the jet exit velocity U_0. The intermediate merging zone extends up to reattachment of the annular jet at the central axis, where $\partial u/\partial r = 0$. Flows of the outer and inner mixing regions are merged there together (the axis of the potential core and its associated high velocities disappears at the jet's central axis). The fully merged zone occurs further downstream from the reattachment point. In this zone, after some developed distance, velocity profiles of the annular jet are self-similar and similar to a jet issuing from a round nozzle. Additionally, velocity profiles have a

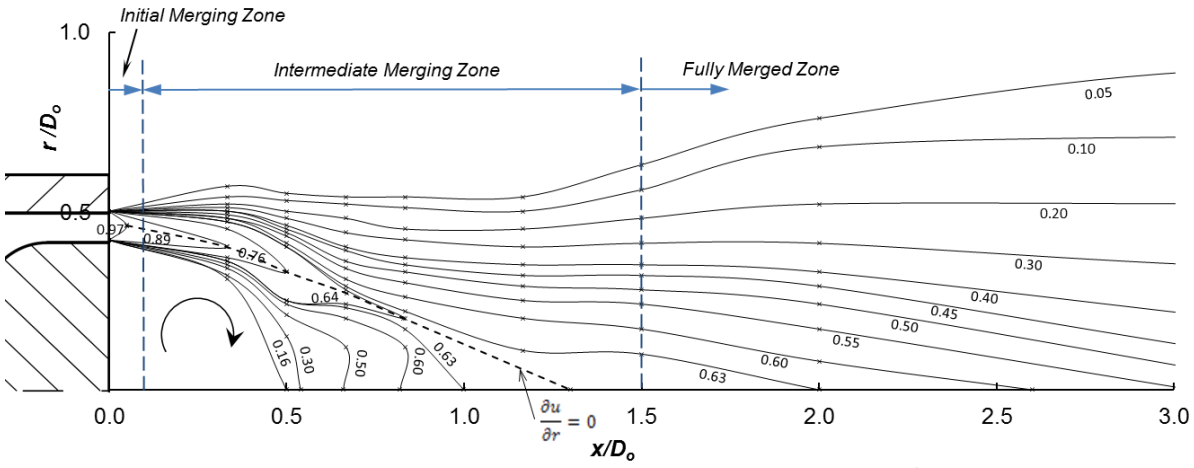

Fig. 3. *Time mean annular jet (Nozzle A - D_i/D_o = 0.84, U_{AV} = 9 m.s^{-1}, Re_D = 17,000).*

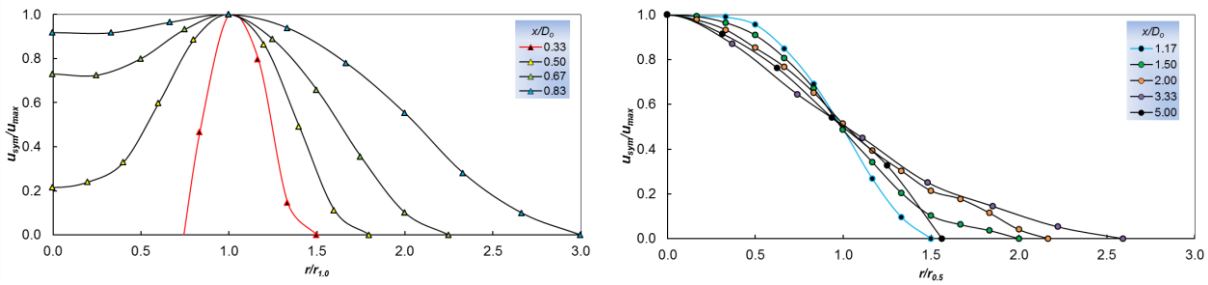

(a) (b)

Fig. 4. *Velocity profiles of time-mean annular jet (Nozzle A, Re_D = 17,000): (a) Intermediate merging zone, (b) End of intermediate merging zone and fully merged zone.*

single peak at the central axis in the fully merged zone against the intermediate zone where velocity profiles usually reach two peaks between central axis, *Fig. 4*.

Ko & Chan [7] proved by their experiment that the jet exit velocity does not affect the reattachment position (!) in the investigated Reynolds number range. They also completed data of flow reattachment position. A trend of the reattachment distance x_r with the diameter ratio D_o/D_i was correlated by Trávníček & Tesař [1] and recently updated by Turek et al. [8], *Fig. 6(a)*, in the following equation:

$$\boxed{x_r/D_o = 2.62\,(D_o/D_i) - 1.83} \qquad (2)$$

The reattachment point was found in present study at $x_r/D_o = 1.3$ for the *Nozzle A* - $D_i/D_o = 0.84$, $U_{AV} = 9\ m.s^{-1}$ and $Re_D = 17{,}000$.

4. Flow Field Patterns

The *bistability* in fluid mechanics is defined by the existence of two stable steady states, when the boundary conditions alone cannot determine uniquely which of these two states takes place. The character of the flow depends on the previous history of parameter changes. The closely related term *hysteresis* is used to describe the response to a quasi-steady change of one of the parameters, characterized by a different response of the system when this parameter is increased or decreased. The relationship between the parameters forms the so called *hysteresis loop*.

Annular IJs, dependent on the nozzle-to-wall distance, may have bistable character and exhibit at least two different main flow field patterns – as shown by Trávníček & Tesař [1, 2]:

"A" pattern is characterized by the small recirculation region (bubble) of separated flow, which is located just downstream from the nozzle centerbody. Jet impingement onto the wall is similar to that of common round IJs, i.e. the stagnation point is located in the cross-section of the nozzle axis with the wall;

"B" pattern exhibits a large recirculation area of separated flow reaching up to the impingement wall. Instead of the stagnation point of *A* pattern, there is a stagnation circle. The entire space between the nozzle exit's inner diameter and the stagnation circle is filled with the recirculating fluid.

Between these two main flow field patterns there can exist even more flow field patterns – e.g. Tesař & Trávníček [3] discussed annular IJs in which five (!) flow regimes were identified by a numerical simulation.

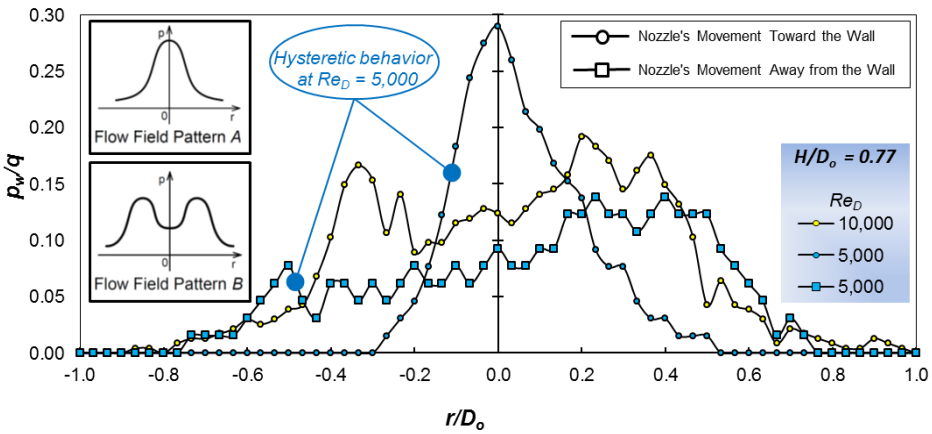

Fig. 5. *Wall pressure at the nozzle-to-wall distance $H/D_o = 0.77$ (Nozzle C_{EXT} - $D_i/D_o = 0.95$ with extension $E = 3.5$ mm).*

The *hysteresis* is considered by the structural view point [8] in this study. Wall pressure measurements at varied nozzle-to-wall distances are shown in *Fig. 5* and *Appendix*. The hysteretic behavior showed up for the nozzles of $D_i/D_o = 0.95$ at small Reynolds number $Re = 5{,}000$. Evidently, the nozzle centerbody extension in nozzles with small annular slot width at low Reynolds numbers makes the hysteresis loop to move closer to an impingement wall. Also, it may cause the area of hysteresis larger.

A significant change of the flow field structure in annular IJs, from small (*pattern A*) to large recirculation zone (*pattern B*) or vice versa (movement dependency between nozzle and wall), is characterized by the so called "*critical value*" of the nozzle-to-wall distance. At this nozzle-to-wall position, two of the most distinctive states of annular IJs border on each other [1]. Trávníček & Tesař [1] correlated the critical value by equation presented in *Fig. 6(b)*. The new equation for critical value estimation was made, *Fig. 6(b)* (values were gained from the pressure dependencies presented in *Appendix*), in the following form:

$$x_c/D_o = 1.77\,(D_o/D_i) - 0.91 \qquad (3)$$

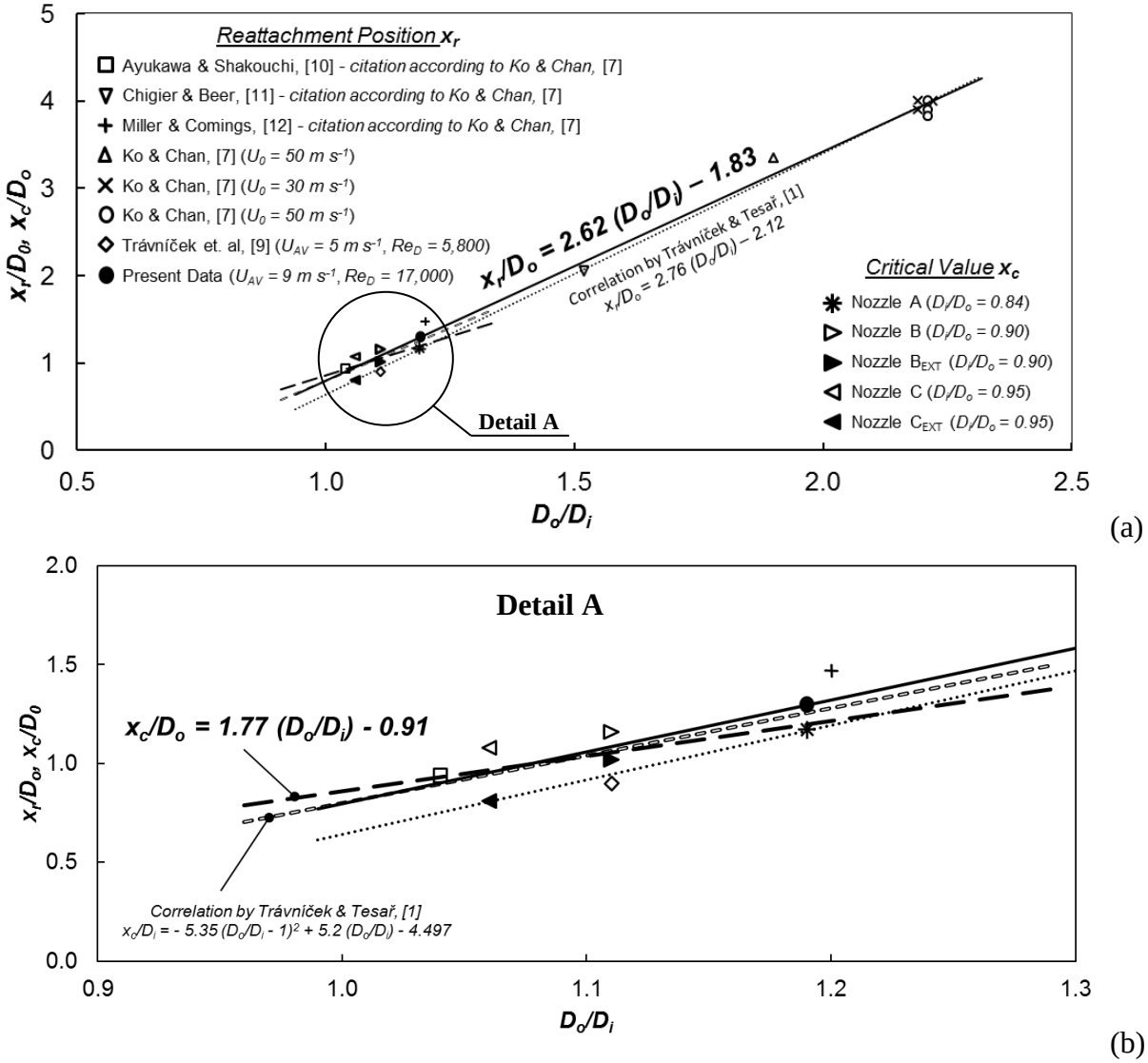

Fig.6. *(a) Reattachment position with diameter ratio, (b) Critical value of nozzle-to-wall distance with diameter ratio.*

5. Conclusions

The estimation of reattachment position for annular jets was updated by the correlation equation. Moreover, the new equation of critical value estimation for annular impinging jets was accomplished.

According to our expectation based on previous papers and supported by this investigation, the bistability and hysteresis are promoted by decreasing the Reynolds number, decreasing the width of the annular nozzle slot, and by the extension of the nozzle centerbody.

Acknowledgment

The authors gratefully acknowledge the support of the GAASCR grant Nr. IAA 200760801 and Grant Agency of the Czech Republic grant Nr. P101/11/J019.

List of Selected Symbols

b	Annular Slot Width, $b = (D_o-D_i)/2$	[m]
D_E	Diameter of Nozzle Extension	[m]
D_i	Inside Diameter	[m]
D_o	Outside Diameter	[m]
E	Length of the Nozzle Extension	[m]
H	Nozzle-to-Wall Distance	[m]
l_{FM}	Length of Scale on the Rotameter's Tube (Flow Rate Measurement)	[m]
p_w	Pressure on the Wall	[Pa]
p_{w0}	Stagnation Pressure on the Wall	[Pa]
q	Dynamic Pressure for Incompressible Fluid, $q = (1/2)\,\rho\,U_{AV}^2$	[Pa]
Q_b	Flow Rate of System Output	$[m^3.s^{-1}]$
r	Radial Distance from Jet Axis	[m]
$r_{0.5}$	Half of Radial Distance to Maximum Velocity of Velocity Profile (1 peak)	[m]
$r_{1.0}$	Radial Distance to Maximum Velocity of Velocity Profile (2 peaks)	[m]
Re_b	Reynolds Number based on the Annular Slot Width	[1]
Re_D	Reynolds Number based on the Outside Diameter	[1]
U_0	Jet Exit Velocity	$[m.s^{-1}]$
U_{AV}	Average Velocity of Jet from the Annular Nozzle	$[m.s^{-1}]$
u_{max}	Maximum Velocity of Velocity Profile	$[m.s^{-1}]$
u_{sym}	Symmetric Velocity of Velocity Profile	$[m.s^{-1}]$
x	Axial Distance from the Nozzle Exit	[m]
x_r	Distance to the Point of Reattachment	[m]
x_c	Distance to the Critical Value	[m]
ν	Kinematic Viscosity of Air at Laboratory Conditions	$[m^2.s^{-1}]$
π	Mathematical Constant	[1]
ρ	Density of Air at Laboratory Conditions	$[kg.m^{-3}]$

References

[1] Trávníček Z., Tesař V.: Annular Impinging Jet with Recirculation Zone Expanded by Acoustic Excitation. Int. Journal of Heat and Mass Transfer, Vol. 47, No. 10, pp. 2329-2341, 2004

[2] Trávníček Z., Tesař V.: Hysteretic Behavior of Annular Impinging Jets. 5th European Thermal-Sciences Conference, The Netherlands, May 18-22, JET 6, pp. 186-187, 2008

[3] Tesař V., Trávníček Z.: Increasing Heat and/or Mass Transfer Rates in Impinging Jets. Journal of Visualization, Vol. 8, No. 2, pp. 91-98, 2005

[4] Trávníček Z., Peszyński K., Hošek J., Wawrzyniak S.: Aerodynamic and Mass Transfer Characteristics of an Annular Bistable Impinging Jet with a Fluidic Flip-Flop Control. International Journal of Heat and Mass Transfer, March, Vol. 46, No. 7, pp. 1265-1278, 2003
[5] Maršík F, Trávníček Z., Novotný P., Werner E.: Stability of Swirling Annular Flow. Journal of Flow Visualization and Image Processing, Vol. 17, No. 3, pp. 267-279, 2010
[6] Aalborg Instruments Inc.: Rotameters AALBORG – Technical Information, pp. 13-14 and p. 35, 2002
[7] Ko N. W. M., Chan W. T.: Similarity in the Initial Region of Annular Jets: Three Configurations. J. Fluid Mech., Vol. 84, part 4, pp. 641-656, 1978
[8] Turek T., Trávníček Z., Šafařík P., Tesař V.: Annular Jets and Annular Impinging Jets. Topical Problems of Fluid Mechanics 2012, pp. 105 -108, 2012. ISBN 978-80-87012-40-6
[9] Trávníček Z., Werner E., Maršík F., Kordík J., Šimurda D.: Swirling Annular Impinging Jets with Hysteretic Behavior. Turbulence, Heat and Mass Transfer 6, Begell House Inc, pp. 497-500, 2009
[10] Ayukawa K., Shakouchi T.: Analysis of a Jet Attaching to an Offset Parallel Plate. Bull. Japan Soc. Mech. Engrs 19, pp. 395-401, 1976
[11] Chigier N. A., Beer J. M.: The Flow Region Near the Nozzle in Double Concentric Jets. Trans. A.S.M.E., J. Basc Engng 86, pp. 794-804, 1964
[12] Miller D., Comings E. W.: Force-Momentum Fields in a Dual-Jet Flow. J. Fluid Mech. 7, pp. 237-256, 1960

Appendix

Annular Impinging Jets – Characteristics of Nozzles

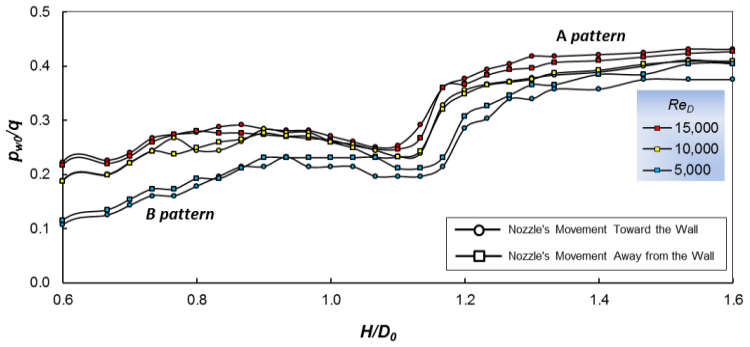

(a)

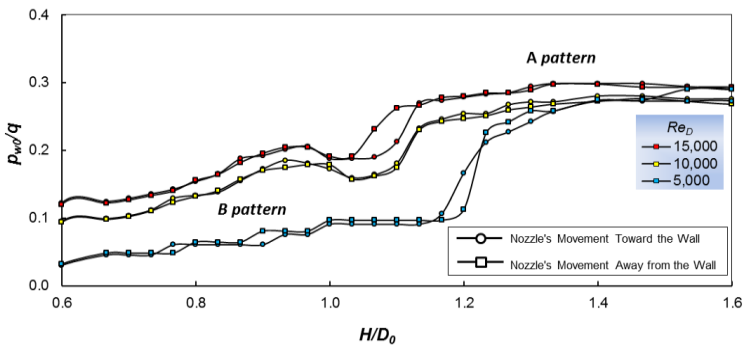

(b)

Fig. 7(a-b). *For legend see Fig. 7(c-e).*

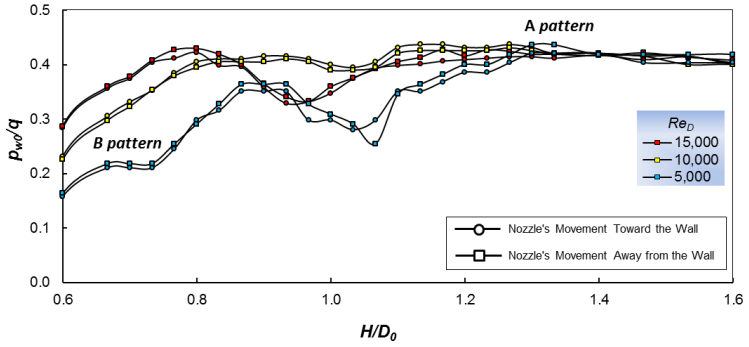

(c)

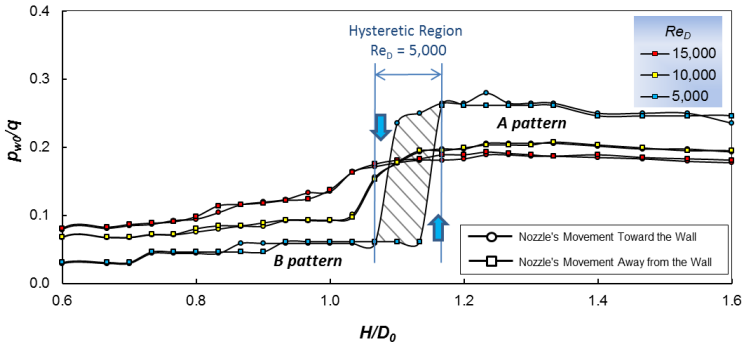

(d)

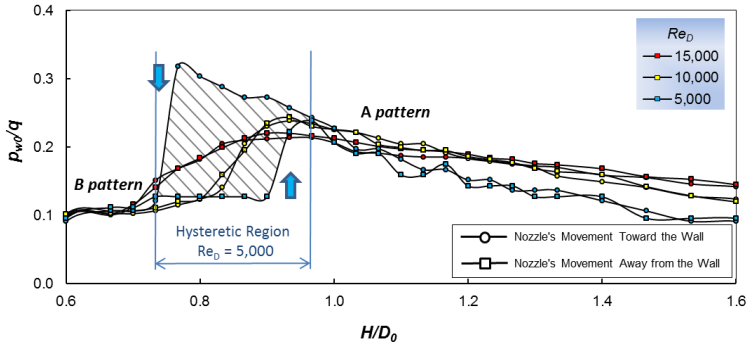

(e)

Fig. 7(c-e). *Dimensionless stagnation pressure in the central point on the wall (r=0) as a function of the relative nozzle-to-wall distance for the nozzles: (a)* ***A*** *- D_i/D_o = 0.84, (b)* ***B*** *- D_i/D_o = 0.90, (c)* $\boldsymbol{B_{EXT}}$ *- D_i/D_o = 0.90 with E = 5 mm, (d)* ***C*** *- D_i/D_o = 0.95, (e)* $\boldsymbol{C_{EXT}}$ *- D_i/D_o = 0.95 with E = 3.5 mm.*